

Improved optical techniques for studying sonic and supersonic injection into Mach 3 flow

A.E. Buggele and R.G. Seasholtz
NASA Lewis Research Center
Cleveland, OH 44135

ABSTRACT

Filtered Rayleigh Scattering and shadowgraph flow visualization were used to characterize the penetration of helium or moist air injected transversely at several pressures into a Mach 3 flow in the NASA Lewis 3.81 inch by 10 inch continuous flow supersonic wind tunnel. This work is in support of the LOX (liquid oxygen) Augmented Nuclear Thermal Rocket program. The present study used an injection-seeded, frequency doubled Nd:YAG pulsed laser to illuminate a transverse section of the injectant plume. Rayleigh scattered light was passed through an iodine absorption cell to suppress stray laser light and was imaged onto a cooled CCD camera. The scattering was based on condensation of water vapor in the injectant flow. Results are presented for various configurations of sonic and supersonic injector designs mounted primarily in the floor of the tunnel. Injectors studied include a single 0.25 inch diameter hole, five 0.112 inch diameter holes on 0.177 inch spacing, and a 7° half angle wedge. High speed shadowgraph flow visualization images were obtained with several video camera systems. Roof and floor static pressure data are presented several ways for the three configurations of injection designs with and without helium and/or air injection into Mach 3 flow.

1. INTRODUCTION

The advent of demonstrating the technical maturity of future engine systems for space launch, from ground to orbit, and from orbit back to ground requires development of additional non-intrusive instrumentation systems and techniques. Fuel injection strategies used in LOX Augmented Nuclear Thermal Rocket (LANTR) and Rocket Based Combined Cycle (RBCC) Strutjet development require optimization through extensive experimentation in direct connect free jet tests. What is required is to provide design information by obtaining qualitative data with new supersonic wedge geometry injectors that reduce the wall heat flux near the injector while avoiding the classic separation bubble in front of a normal jet associated with the standard-baseline sonic hole (underexpanded) injection. The goal is to reduce the injection hot spots common with old injector designs while reducing the cooling system complexity within the engine ducting^{1,2,3}. This study continues the preceding study by the authors⁴. Rayleigh scattering (RS), shadowgraph, and static pressure data are presented using optical access windows⁴ while injecting moist air or helium. A related paper⁵ describes the technique used in this study to improve the effectiveness of the iodine absorption cell to suppress stray scattered laser light. It was shown that an etalon placed in the laser oscillator cavity significantly improved the performance of the iodine cell by eliminating low level 40 GHz bandwidth light from the injection-seeded Nd:YAG laser output.

The present investigation of plume penetration into the SWT's mainstream with vortex enhancement adds to the baseline of design data to increase the efficiency of the injection (mixing) process while minimizing large blocking/bow plume shocks with their large stagnation pressure loss. Development of non intrusive instrumentation systems and techniques is required to characterize not only generated plumes of various injectants, but also to validate the injection nozzle designs and/or to assist in the development of innovative (specific Mach no.) injector nozzles for fully developed or partially developed supersonic flows. This latter case is typical of the requirements associated with the LANTR program, where injection will occur relatively close to the rocket's throat (e.g., see fig. 5 of ref. 2).

The goal of the test program is to investigate injection, penetration, and mixing dynamics of three different injector designs. Further inspection of prior random the pulsed light source shadowgraphs shown in reference 5 revealed several series of dynamic/unsteady flow phenomena occurring within the generated plumes.

2. EXPERIMENT

Three different types of test injectors were mounted in the NASA Lewis 3.81 inch (width) by 10.00 inch (height) continuous flow SWT (fig. 1a). [The initial test hardware, designated Configuration (Config.) No. 1, consisted of 0.25 inch diameter sonic hole injection ports mounted in the tunnel roof and floor, with the leading edge of the holes located 1.85 inches downstream of the SWT nozzle exit plane.] Fifty seven static pressure measurement ports were located about the injection site, with the same position pattern for all configurations. All static holes are located on 0.125 inch spacing or increments. A second injector was installed 6.0 inches downstream from Config. 1; it consisted of either five 0.112 inch diameter sonic holes on 0.177 inch spacing (called Config. 2), or a 7° half angle supersonic wedge injector (called Config. 3). The tunnel inlet total pressure was nominally 42.5 psia, with an exit pressure less than 1.5 psia for all conditions presented. The majority of injector total pressure testing occurred at a matching pressure of 42.5 psia with moist air or helium as the injectant into Mach 3 flow. However, injection having total pressure ranging between 22.5 psia and 62.5 psia was also studied, providing some very interesting dynamic shadowgraph flow visualization images and injection (mixing) process phenomena.

Two flush mounted piezoresistive pressure transducers were installed 0.30 and 2.55 inches downstream of the Config. 3 (wedge) injector in an attempt to obtain specific frequency spectrum signatures for all future injector and/or injectant configurations. A Lewis designed and fabricated miniature 0.250 inch wide 25° wedge probe provided flow angle data within the plume's internal structure at eleven 0.250 inch diameters downstream from the origin of injection (see fig. 2a & 2b).

The Config. 3 (wedge) injector having a length of $L = 0.82$ inches was instrumented with three 0.020 inch diameter static taps located at 0.15L, 0.50L, and 0.85L; these taps were located in the injector nozzle 0.030 inches below the tunnel's flow surface. Calculated injector Mach no. was obtained from an electronically scanned pressure measurement system. Planar plots of static pressure measurements in the vicinity of the injection sites are also shown in (Fig. 1b). Other methods of presenting these pressure distributions using a 3-D graphics package are also shown herein and in a NASA TM that contains more extensive results⁶.

One objective was to develop techniques for obtaining quantitative measurements of the mole fraction of helium or higher molecular weight gases injected from one or more injectors into the supersonic air flow. However, without a large pressure regulated source of injectant gas supply, performing RS measurements can be difficult under the best controlled conditions. The helium supply (when used) consisted of four standard 220 scf gas cylinders. This arrangement provided less than 40 seconds of helium flow through a single injector when 62.5 psia total pressure conditions were required. Helium injection through multiple and/or several injectors significantly decreased the RS data gathering time while providing inadequate time to obtain consistent injectant conditions. This activity was temporarily abandoned in favor of moist air injectant because it provided essentially infinite run time. Since the mainstream flow in the LANTR engine will use 3500° hydrogen with LOX as an injected oxidizer near the rockets throat, more precise RS measurements and experiments need to be eventually performed. Injecting higher density gases such as Xenon (with a molecular weight of 131) into ambient or moderately heated air should be investigated in order to confirm diffusion mixture efficiencies with previous injector evaluations and to identify potential hot spots by measuring static pressure distribution.

3. RAYLEIGH SCATTERING MEASUREMENTS

The beam from an injection-seeded, frequency-doubled Nd:YAG laser (0.7 J, 532 nm, 10 Hz pulse rate, 8 ns pulse duration) was formed into a sheet about 1.5 inches high, which was passed through the 47 inch long, 1.2 inch thick, full roof-to-floor windows. The windows are plate glass, with a relatively large number of included bubbles. These windows have been in use for a number of years, and their inner surfaces have been abraded by particle impacts. In addition, some damage was caused by the high power pulsed laser in earlier tests. These poor quality surfaces resulted in a large amount of laser scattering. Light was collected at 45° to the beam direction, passed through an iodine cell, and imaged onto the liquid nitrogen cooled CCD array (1752x532 pixels, 70% quantum efficiency) with a 85 mm focal length, f/1.4 lens. This resulted in a pixel viewing a region on the laser sheet 0.10 mm high by 0.14 mm wide (the width being larger because of the oblique viewing angle). The oblique viewing angle caused keystone distortion, and

the limited depth of focus caused a significant blurring of particle images, which made it difficult to effectively remove them. As a result of these factors, the spatial resolution of the measurement was only about 1 or 2 mm. Only a fraction of the total CCD array was used (about 350x350 pixels) to reduce the storage requirements and the time to transfer data from the camera to the computer. The laser and optics were mounted on a remotely controlled 3-axis positioning system, which was used to position the laser sheet at the desired axial locations. All image data were taken in groups of 20 for both single-shot and 10-shot exposures. This allowed time averages to be calculated based on 200 shots.

4. SHADOWGRAPH FLOW VISUALIZATION

A shadowgraph system was also used to visualize the flow. The double pass shadowgraph system used a 30 inch diameter concave surface mirror and a 16 inch by 24 inch front surface flat mirror that was $\frac{1}{8}$ inch thick (for the initial testing) and a 16 inch diameter optical flat mirror 2 inches thick (for later tests). Two techniques were used to record shadowgraph images. The first technique used a continuous light source and a gated (10 μ s) intensified CCD camera with an RS170 output. These images were recorded on a VCR and provided a continuous visualization of the flow. Video images were obtained using two cameras. One video camera had a 30 frames per second (f/s) rate, and the other had a 1000 f/s or more rate. Best video record quality during injection was obtained with a 10 μ s shutter setting for both video cameras. A computer frame-grabber could also be used to capture these images with an data acquisition overlay providing actual injectant pressure decay over time.

The second technique used a 35-mm camera (f/2.8, 135 and 180 mm focal length lenses with 1/2000 sec exposure for continuous light, or 1/250 second exposure for pulsed light). These images were of a higher quality than the VCR recorded images. Figure 2 shows typical injector plume shadowgraph images obtained with the 35-mm camera for 42.5 psia (nominal) matched total tunnel pressure helium or moist air injectants (also 22.5 to 62.5 psia) into Mach 3 flow.

5. EXPERIMENTAL RESULTS

Figure 1b shows some typical individual injector plume centerline floor static pressure distributions, with a helium injected at 56.3 psia for Config. 1 (0.25 inch sonic hole), followed by 41.8 psia for Config. 2 [(5) 0.112 inch sonic holes], and 62.8 psia for Config. 3 (7° half angle supersonic wedge) injector, respectively. This figure also compares calculated Mach no. relative to the wedge injector's length L at .15L, .5L, and .85L for air and helium injectants; at pressures of nominally 22.5, 42.5, and 62.5 psia (L=0.821 inches). As expected, the Config.3 (wedge) Mach number at .5L did not vary when pressure was increased from 22.5 psia to 62.5 psia with either injectant. However, the Mach number did vary about 20% with air and about 25% with helium between positions .15L and .85L.

Typical pulsed light source shadowgraph photographs shown in Figure 2 reveal the primary plume flow differences between the three configurations with the same tunnel and injectant total pressure (42.5 psia) with or without injection (Fig. 2c to 2f). Figure 2g shows the effect of multiple tandem floor 56.3 psia helium injection by Config. 1 and 2 generating a 70% penetration improvement over single equivalent Config. 1 and 2 injection. A slightly further penetration improvement appears to occur with triple injection (see Figure 2h.). These observations were made using the trailing edge of the wedge probe's sting support as a reference location. For Config. 3 (7° half angle wedge) plume images; Figure 2f, 2i, and 2j random shadowgraphs show progressively farther penetration as the air injection pressure was increased. Gruber et al⁷ have reported similar findings at Mach 2 using planar scattering with circular 90°, circular 15°, and elliptical 90° injectors and helium or carbon dioxide as injectants.

The cross/circled regions of Figures 3a to 3c sequential high speed (1000 f/s) video shadowgraph plume image frames of 42.5 psia helium being injected from a Config. 3 (wedge) reveal the existence of an eddy formation. The eddy's center is nominally 1.1 inches above and 1.1 inches behind the wedge injector's nozzle exit, or approximately 9.8 inches downstream of the SWT's nozzle-exit. Figure 3c shows frame 960, where the eddy appears to have burst and moved further downstream approximately 1.1 inches. Reviewing the entire reading no. [RDG 77] 5000 frame video record, less than 5% of the frames show the existence of any eddy being regenerated, fully developed, or in the process of decay (bursting). This eddy phenomenon becomes more common and lasts longer as injection pressure is reduced.

Figure 3e shows several single injector centerline flow static pressure distributions for 42.5 psia matched total tunnel pressure to helium or air transverse injection into Mach 3 flow. For ease of comparison, all injector configurations are plotted over each other, regardless of whether their origin was at 1.85 or 7.85 inches from the nozzle exit plane. Config. 2 shows a clear improvement over Config. 1's strong bow shock. The isolated static measurement located at 8.375 inches for the Config. 2 plot is due to a 0.020 inch static tap in between two 0.112 inch sonic holes. The extreme variation in Config. 3's pressure plot at the 10.0 inch region is due to the fixed position/structure of vortices at that point.

Figure 4 (a-c) of Config. 3 (wedge) and Figure 4 (e-f) of Config. 1; matched air injection to tunnel total pressure static pressure plots; 0°, 40°, and -140° views reveal the significant pressure distribution differences between the two. The forward pressure wave of Config. 1 can be likened to the blunt bow wave of a slowly moving barge being pushed by a tugboat. Config. 3 (wedge) created a 45° rear swept bow wave pressure distribution similar to the bow wave generated by a 35 foot cabin cruiser moving at 20 knots. Also produced is a large stern wave/wake. Figures 4d and 4h reveal greater pressure differences with the injection of 62.5 psia air as shown in the -140° view about the X-axis. The plots identify the values of the individual static pressure ports as either peaks or valleys in its interpolated representation. Note that the interpolated values between the peaks do not represent measurements.

Figure 5 shows similar pressure distribution results for single 42 psia helium injection when plotting Config. 1, 2, and 3; 40°, and -140° view data and the effect of dual floor 56.3 psia helium injectant data for Config. 2 [when Config. 1 plume is activated in front of Config. 2's plume].

Figure 6 (a-h) sequential high speed (100f/s) video shadowgraph plume images of 22.5 psia helium injection from Config. 3 (wedge) into Mach 2.95 flow per [RDG 80] clearly shows within the highlighted cross-circles a more permanent eddy. The position of this eddy (located as before) was abreast of the trailing edge of the miniature wedge probe sting support. The eddy; appears to reveal itself strongest (the majority of the time) as shown in these sequential frames and other recorded frames on a 120 frame period with a video record speed of 1000 f/s. Also it was hoped that the two flush mounted high response pressure transducers 0.30 and 2.55 inches downstream of the stern of the wedge injector would confirm this basic 8 Hz frequency. The recorded signal levels for the closest transducer were significantly lower than the one further downstream. Both indicated higher broadband signal levels at frequencies less than 100 Hz.

Figure 7a shows the 200 RS image averages of moist air injection from Config. 1 (0.25 inch diameter sonic nozzle) into Mach 3 cross flow at X=2, 3, 4, 5, 6, and 7 inches from the leading edge of the injector. Figure 7b shows Config. 3 (7° half angle wedge) data. At X=2, Config. 3 plume/cross-section is significantly larger than Config. 1. Config. 3 plume/cross-section is approximately 20% larger than Config. 1 when all section cuts are taken in account.

Figures 8a and 8b show 18 random single-shot RS images taken at X=2 inches. Additional data taken at other locations are given in reference 6. The region near the tunnel floor was always visible in the recorded images and reproduced color images. These images provide some qualitative information on the geometry and penetration of the moist air injected into the tunnel flow at the three specific injectant pressures evaluated; nominally 22.5, 42.5, and 62.5 psia.

6. GENERAL DISCUSSION

Shadowgraph images were obtained at the same flow conditions as the RS images, but on a different day. Simultaneous RS and shadowgraph images could not be obtained because the RS optics obscured the field of view of the shadowgraph. Since the Config. 1 injector's datum plane was located upstream of the leading edge of the window by about .80 inches, the shadowgraph images could not show the classic separation bubble in front of the bow shock when injecting. The Configuration 2 bow shock with its forward recirculation pattern caused by the five 0.112 inch diameter sonic hole injection (helium or air) jet is clearly seen, however.

A 4.5 inch long pitot probe containing the miniature 25° wedge that allows flow angle measurements was usually visible in all shadowgraphs 1.75 or 5.0 inches from the SWT's roof. This miniature probe appeared to have no effect on

the static pressure distribution of Config. 2 and 3 plumes data when extended 1.75 or 5.0 inches into the flow. When matched 42.5 psia moist air was being injected from the roof [Config. 1 (0.25 inch) sonic hole] into Mach 2.95 flow, the measured flow angle within the plume, indicated 0.00° for D between 0.30 and 1.00 inches. However, at D =1.10 inches, the flow angle just outside the plume, but behind the generated bow shock, measured 1.42°, and, at D =1.50 inches, 1.70°.

The momentum flux ratio, a parameter commonly used to characterize penetration of a jet into crossflow, is defined as

$$J = \frac{\gamma_{inj} P_{inj} M_{inj}^2}{\gamma_{tun} P_{tun} M_{tun}^2}$$

where the subscripts refer to the tunnel flow (_{tun}) and the injectant flow (_{inj}). The momentum flux ratios for the various test conditions are shown in the table. The wedge static pressures were taken from the center tap in the injector (shown in fig. 1). The static pressure for the 0.25 inch hole was calculated from the total pressure assuming isentropic flow⁸.

$$M = \left\{ \frac{2}{\gamma - 1} \left[\left(\frac{P_T}{P} \right)^{\frac{\gamma - 1}{\gamma}} - 1 \right] \right\}^{1/2}$$

where PT is the total pressure, P is the static pressure, and γ is the ratio of specific heats (1.4 for air and 1.66 for helium). The tunnel total pressure was taken as 42.5 psia for all cases.

Wedge

| Injectant | P total (psia) | P static (psia) | Mach number | J |
|-----------|----------------|-----------------|-------------|------|
| Air | 22.5 | 3.40 | 1.89 | 0.94 |
| Air | 42.4 | 6.57 | 1.87 | 1.79 |
| Air | 62.2 | 9.78 | 1.86 | 2.63 |
| Helium | 23.0 | 2.92 | 1.96 | 1.28 |
| Helium | 41.7 | 5.26 | 1.97 | 2.32 |
| Helium | 63.8 | 8.92 | 1.90 | 3.65 |

0.25 inch sonic hole

| Injectant | P total (psia) | P static (psia) | Mach number | J |
|-----------|----------------|-----------------|-------------|------|
| Air | 22.5 | 11.89 | 1 | 1.14 |
| Air | 42.5 | 22.45 | 1 | 2.16 |
| Air | 62.5 | 33.02 | 1 | 3.17 |
| Helium | 22.5 | 10.98 | 1 | 1.25 |
| Helium | 42.5 | 20.74 | 1 | 2.36 |
| Helium | 62.5 | 30.50 | 1 | 3.47 |

The edge of the helium plume was difficult to determine accurately from random single-shot shadowgraphs because of the dynamic, turbulent nature of the interface between the helium plume and the tunnel flow. The 200 shot Rayleigh scattering average comparisons between Config. 1 and 3, at X/D cuts 2 through 7 inches, show colored visible plume geometry/penetration description data (refer to Fig. 7). Both reveal a kidney shape cross-section. However, the Config. 3 plume separates into two distinct vortices-cells, which appear to divide into more cells vertically as RS cuts move farther downstream. When using all of Figure 7 200 RS shot average plume height and width comparisons, Config. 3 plume appears to be larger than Config. 1 plume indicating better mixing by approximately 20%. This finding is confirmed, to a lesser degree (about 10 percent), by the 18 random single shot RS images of Figure 8 when comparing (8a -Config. 1) to (8b -Config. 3) X = 2 inch data. The apparent difference in plume size when comparing RS 200 shot average to 18 random single shot RS data may simply be the lack of single shot images available for a accurate comparison to establish mixing efficiency gain. This data adds to the baseline information obtained by Gruber et al⁷ and Barber et al⁹ with injected helium or carbon dioxide for injection nozzles similar to these.

7. CONCLUDING REMARKS

This work demonstrated the feasibility of using single shot filtered Rayleigh scattering to characterize the unsteady plumes created by injecting moist air from several injector designs into a Mach 3 flow. The static pressure distributions for the forgoing configurations revealed not only the differences between injector designs, but the result of dynamic turbulence on possibly predicting hot-spot locations associated with a specific injector geometry. Since the present high speed video recordings identified the existence of an eddy within the plume created by Configuration 3 (7° half angle wedge), further study of this phenomenon is warranted. This requires software and modifications to couple a higher speed (eight frames at 100 kHz or higher rate) camera system to a rapid sequential pulsed light source in order to trace the growth and movement of these eddies.

The future test plan will emphasize the unsteady characteristics associated with a variety of injector designs including multiple inline arrays of round sonic and supersonic nozzles and innovative wedge-shaped injectors. These injectors will be located in the tunnel roof and floor modules, both downstream of the tunnel nozzle exit and later in the diverging section of the nozzle. Newly installed static pressure ports at the exits of all injector designs geometry will provide comparison performance data to industry (Mach number, mass flow, Reynolds number, density static temperature, etc.). A large capacity gas storage supply will be installed. This will allow much more efficient use of test run time compared to the use of the 220 scf cylinders used in this work, and will allow the study of larger momentum flux ratios for future injection design development. Also, use of better quality fused silica windows and frames that are already fabricated will provide additional research options for all future tests (such as operation in the ultraviolet using the Nd:YAG 266 nm fourth harmonic, where RS measurements have greater signal-to-noise ratio). These new windows will also have a much better surface quality, which will result in a significant reduction in the amount of stray scattered laser light. In addition, these windows will be mounted such that they can quickly be removed for cleaning. (The windows used in this work require a full day to remove and replace.)

8. ACKNOWLEDGEMENTS

We would like to acknowledge the efforts of Mr. W. Trevor John and Mr. Bertram Floyd, who were responsible for setting up and aligning the Rayleigh scattering optical system used for this work, Mr. Richard Senyitko and Mr. Salvatore Giordano, who were responsible for the wind tunnel preparation, Mr. Kenneth Weiland, who was responsible for setting up the shadowgraph system, Mr. Barry Wilson and Mr. Robert Everett who fabricated the injector parts and/or modules, Mr. Roger Meredith who instrumented the injector parts and modules, and Mr. George Saad who fabricated the 0.25 inch wide 25° wedge probe. Also, we thank Mrs. June Thompson for providing us with computing services, and Mr. Peter Quinn and Mrs. Mary Vickerman for the video supplements. Others worthy of special recognition are Mr. Jim Sims of the Lewis Imaging Technology Center and Mr. Richard Czentorycki of Technical Illustrations.

REFERENCES

1. S.K. Borowski, and B.N. Cassenti, "Nuclear thermal propulsion", *Aerospace America*, p. 49, December 1995.
2. S.K. Borowski, R.R. Corban, D.W. Culver, M.J. Bulman, and M.C. McIlwain, "A revolutionary lunar space transportation system architecture using extraterrestrial LOX-augmented NTR propulsion", *30th Joint Propulsion Conference*, AIAA 94-3343 (NASA TMX-106726), Indianapolis, Indiana, June 27-29, 1994.
3. M.J. Bulman and A. Siebenhaar, "Rocket based combined cycle propulsion for space launch", *46th International Astronautical Congress*, Paper IAF-95-S.5.02, October 2-6, 1995, Oslo, Norway.
4. R.G. Seasholtz and A.E. Buggele, "Study of injection of helium into supersonic air flow using Rayleigh scattering", *35th Aerospace Sciences Meeting & Exhibit*, AIAA 97-0155 (NASA TMX-107409), Reno, Nevada, January 6-10, 1997.
5. R.G. Seasholtz and A.E. Buggele, "Improvement in suppression of pulsed Nd:YAG laser light with iodine absorption cells for filtered Rayleigh scattering measurements", *SPIE Conference on Optical Technology in Fluid, Thermal, and Combustion Flow III* 3172, San Diego, July 27-August 1, 1997.
6. A.E. Buggele and R.G. Seasholtz "Improved optical techniques for studying sonic and supersonic injection in Mach 3 flow", NASA TM 107512 with Video Supplement, July 1997.

7. M.R. Gruber, A.S. Nejad, T.H. Chen, and J.C. Duttons, "Mixing and penetration studies of sonic jets in a Mach 2 freestream, *J. Propul. Power* **11**, March 1995.
8. Ames Research Staff, *Equations, Tables, and Charts for Compressible Flow*, NACA Report 1135, 1953.
9. M.J. Baber, L.A. Roe and J.A. Schetz, "Simulated fuel injection through a wedge-shaped orifice into supersonic flow, 31st AIAA Joint Propulsion Conference and Exhibit July 10-12, 1995, San Deigo. CA, AIAA 95-2559.

Supplement to: *Improved Optical Techniques for Studying Sonic and Supersonic Injection into Mach 3 Flow*

NASA TM 107533 of SPIE paper 3172-52 presented at San Diego, CA; July 31 1997.

3-D Pressure Plot Data Models for Three Injector Designs

| Reading # (RDG) | Injector Configuration | Injection Pressure (PSIA) | Injectant |
|--------------------|---------------------------|------------------------------|-----------|
| 80 | wedge | 22.8 | helium |
| 210 | wedge | 42.5 | helium |
| 2223 | 5-hole | 42 | helium |
| 245 | wedge | 62.3 | air |
| 246 | wedge | 42.6 | air |
| 267 | .25" hole | 42.5 | air |
| 268 | .25" hole | 62.5 | air |

Video clips

RDG 210 vs. 2223

color view [MPEG \(2 MB\)](#) or [Quicktime \(719 KB\)](#)

grid view [MPEG \(2.2 MB\)](#) or [Quicktime \(875 KB\)](#)

RDG 245 vs. 80

color view [MPEG \(1.3 MB\)](#) or [Quicktime \(463 KB\)](#)

grid view [MPEG \(2 MB\)](#) or [Quicktime \(807 KB\)](#)

RDG 246 vs. 267

color view [MPEG \(1.5 MB\)](#) or [Quicktime \(489 KB\)](#)

grid view [MPEG \(3.1 MB\)](#) or [Quicktime \(1.2 MB\)](#)

high speed video shadowgraph plume images

22.4 PSIA air injection wedge [MPEG \(1.4 MB\)](#) or [Quicktime \(819 KB\)](#)

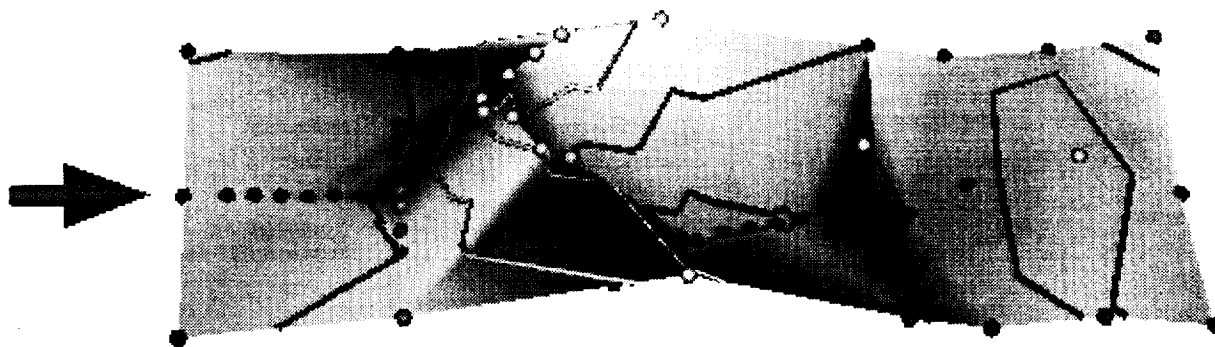
42.5 PSIA helium/air injection wedge [MPEG \(1.7 MB\)](#) or [Quicktime \(986 KB\)](#)

62.6 PSIA helium/air injection wedge [MPEG \(1.6 MB\)](#) or [Quicktime \(907 KB\)](#)

3-D models

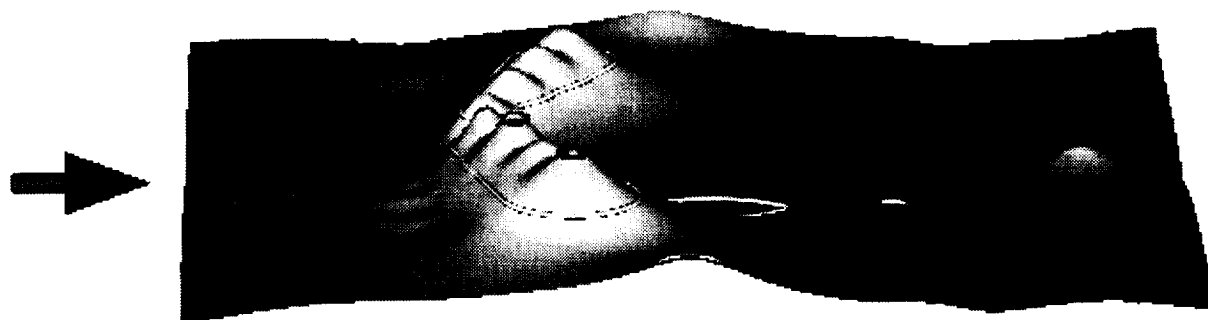
To view the VRML models, you will need a VRML 2 viewer such as [CosmoPlayer](#).

Sparse surfaces



| | | | | | |
|-------------------------|--------------------------|-------------------------|-------------------------|-------------------------|-------------------------|
| RDG 210 | RDG 2223 | RDG 245 | RDG 246 | RDG 267 | RDB 268 |
| (0.7 MB) | (0.7 MB) | (0.7 MB) | (0.7 MB) | (0.8 MB) | (0.9 MB) |

Smoothed surfaces



| | | | | | |
|-------------------------|--------------------------|-------------------------|-------------------------|-------------------------|-------------------------|
| RDG 210 | RDG 2223 | RDG 245 | RDG 246 | RDG 267 | RDG 268 |
| (1.3 MB) | (1 MB) | (1.4 MB) | (1.2 MB) | (1.7 MB) | (1.8 MB) |

For information on the experiment, contact: Alvin.E.Buggele@lerc.nasa.gov phone: (216)433-5561
 For information on the data presentation, contact: Mary.B.Vickerman@lerc.nasa.gov

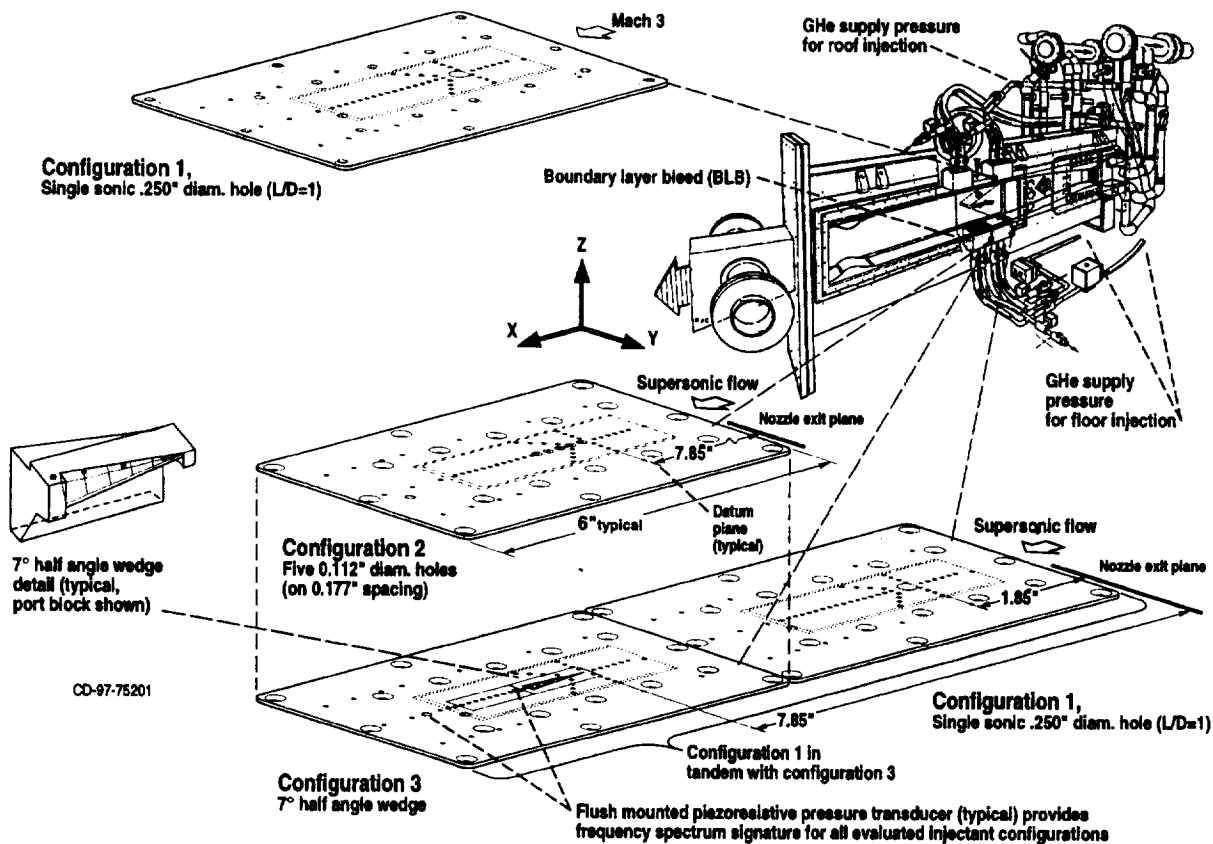


Fig. 1 a. Supersonic wind tunnel with various configurations of injector plates

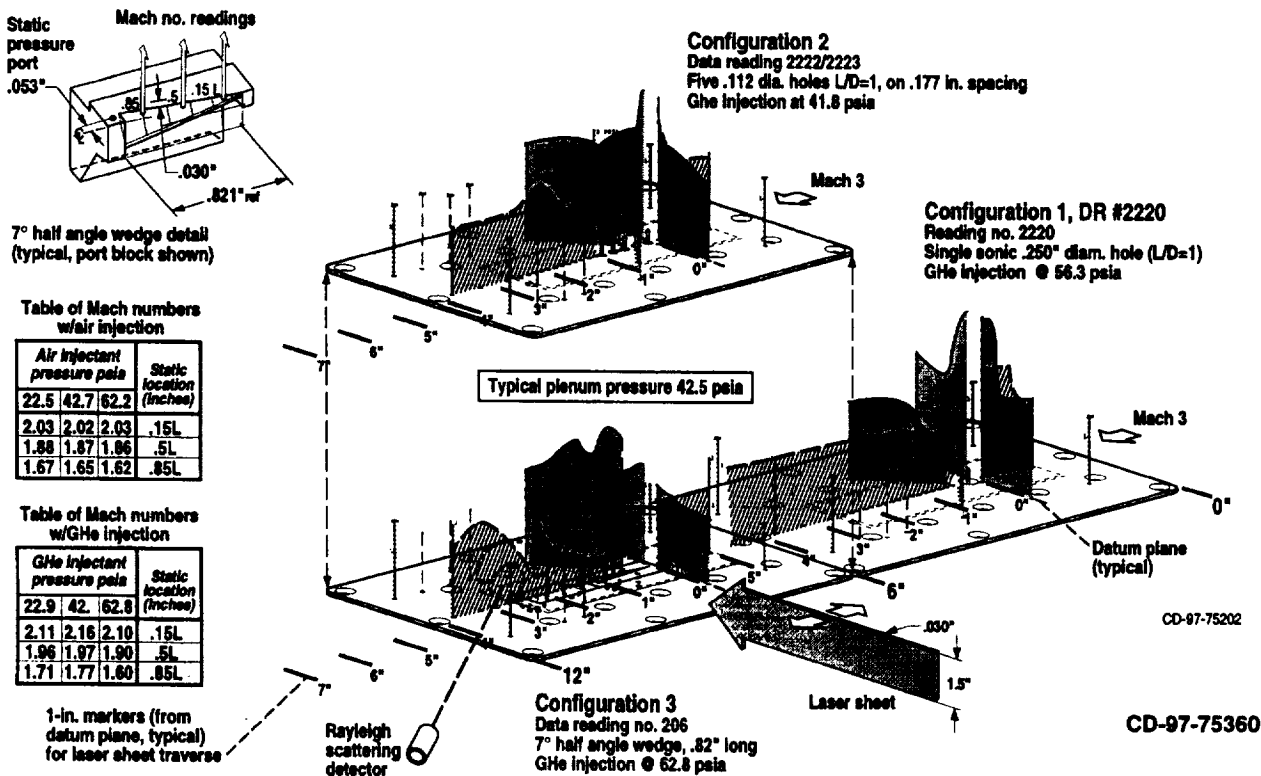
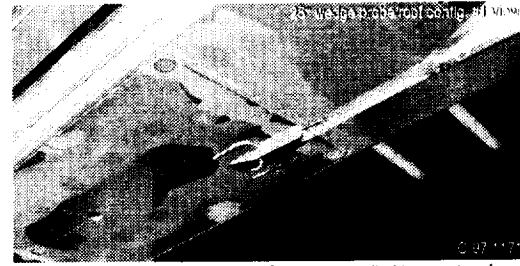


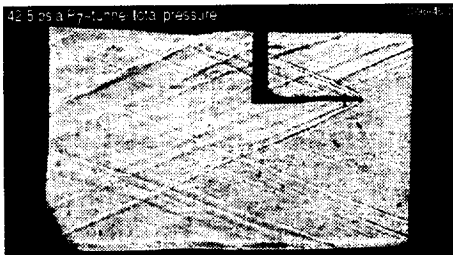
Fig. 1 b. 2-D typical static pressure distributions for GHe injectant at various pressures and configurations of injector plates



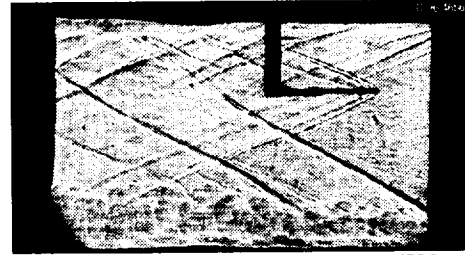
(a) Instrumentation probe/configuration installed in tunnel floor



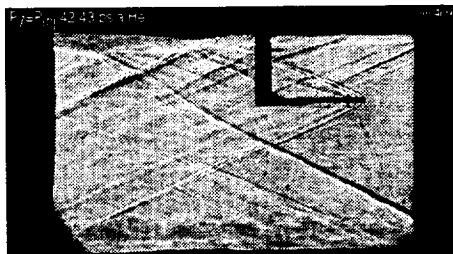
(b) Instrumentation probe/configuration installed in tunnel roof



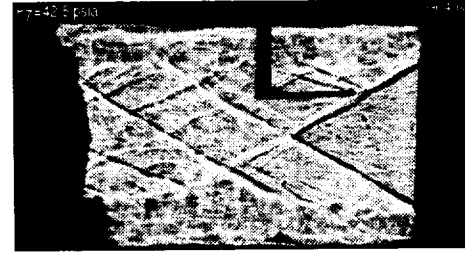
(c) Mach 3 flow shadowgraph w/o injection [RDG #2217/2219]



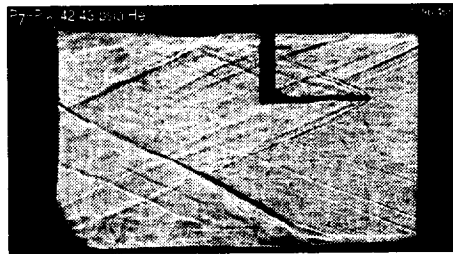
(g) Dual floor 56.3 psia He injection by configs. #1 & #2 [RDG #2220]



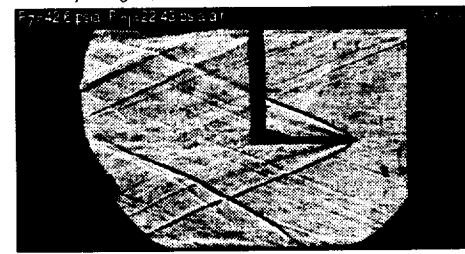
(d) Config #1, .250" hole injection [RDG #2218]



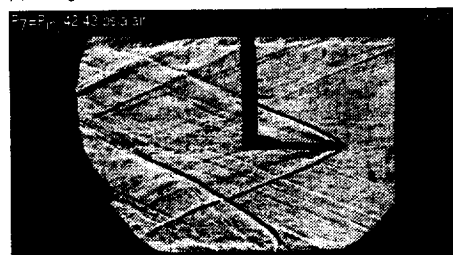
(h) Triple, 62 psia He injection by config #1 on roof & floor and by config #2, 6" downstream on floor [RDG #2195]



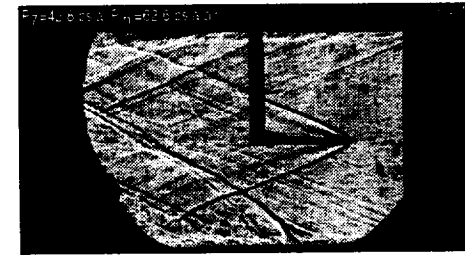
(e) Config #2, five 0.112" diam holes (on 0.177" spacing) [RDG #223]



(i) Config #3 wedge [RDG #189]



(f) Config #3, 7° half-angle wedge [RDG #188]



(j) Config #3 wedge [RDG #187]

CD-97-75361

Fig. 2 - (a-b) Some typical injector configurations installed with SWT instrumentation; (c) typical Mach 3 flow shadowgraph without injection; (d-f) [Config. 1, 2, 3] respectively, with injection for 42-43 psia matched total tunnel/helium (He) or air injection into Mach 3 flow; (g) dual floor 56.3 psia He injection; Config. 1 forward of Config. 2 by 6.0 in.; (h) triple injection, 62 psia He, Config. 1 roof, 1 floor, with Config. 3 6.0 in. downstream (tunnel total pressure at 42.5 psia); (i,j) Config. 3 air injection at 22.4 and 62.6 psia respectively.

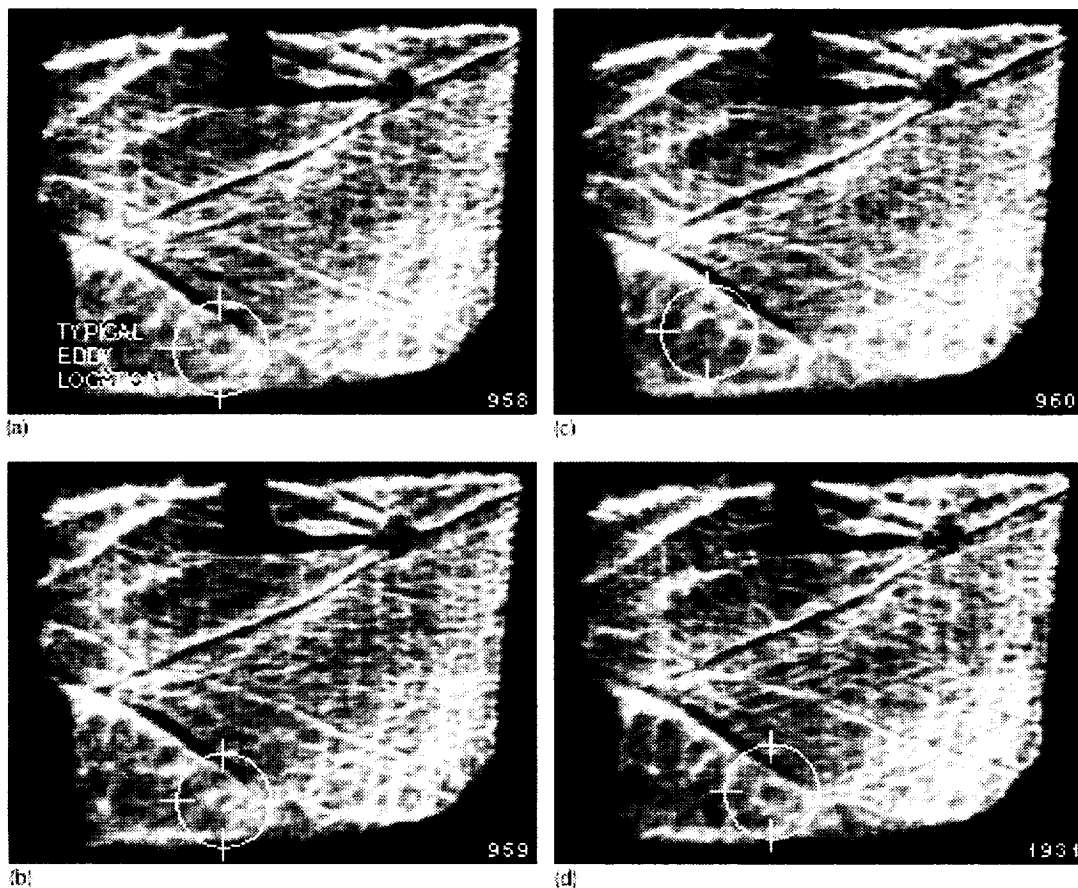


Fig. 3 (a-c) - Sequential high-speed (1000 f/s) video shadowgraph plume images of 42.5 psia helium injection from Config. 3 (wedge) located 7.85 inches downstream of nozzle exit into Mach 2.96 flow [RDG 77]; (d) typical frame No. 1931 showing fully developed eddy in line with trailing edge of probe sting [RDG 77].

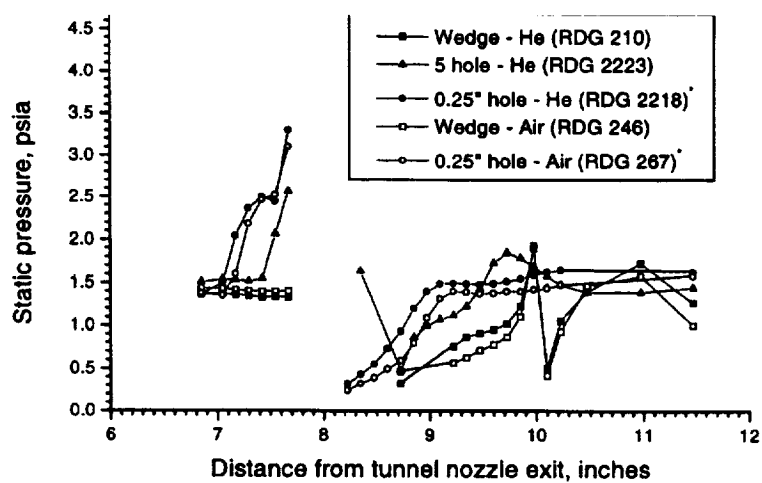


Fig. 3e - Injection plume centerline floor static pressure distribution for 42-43 psia matched tunnel-to-injectant total pressure into Mach 3 flow; * 0.25" hole was located 6 inches upstream from wedge, so subtract 6 inches from x axis for hole data.

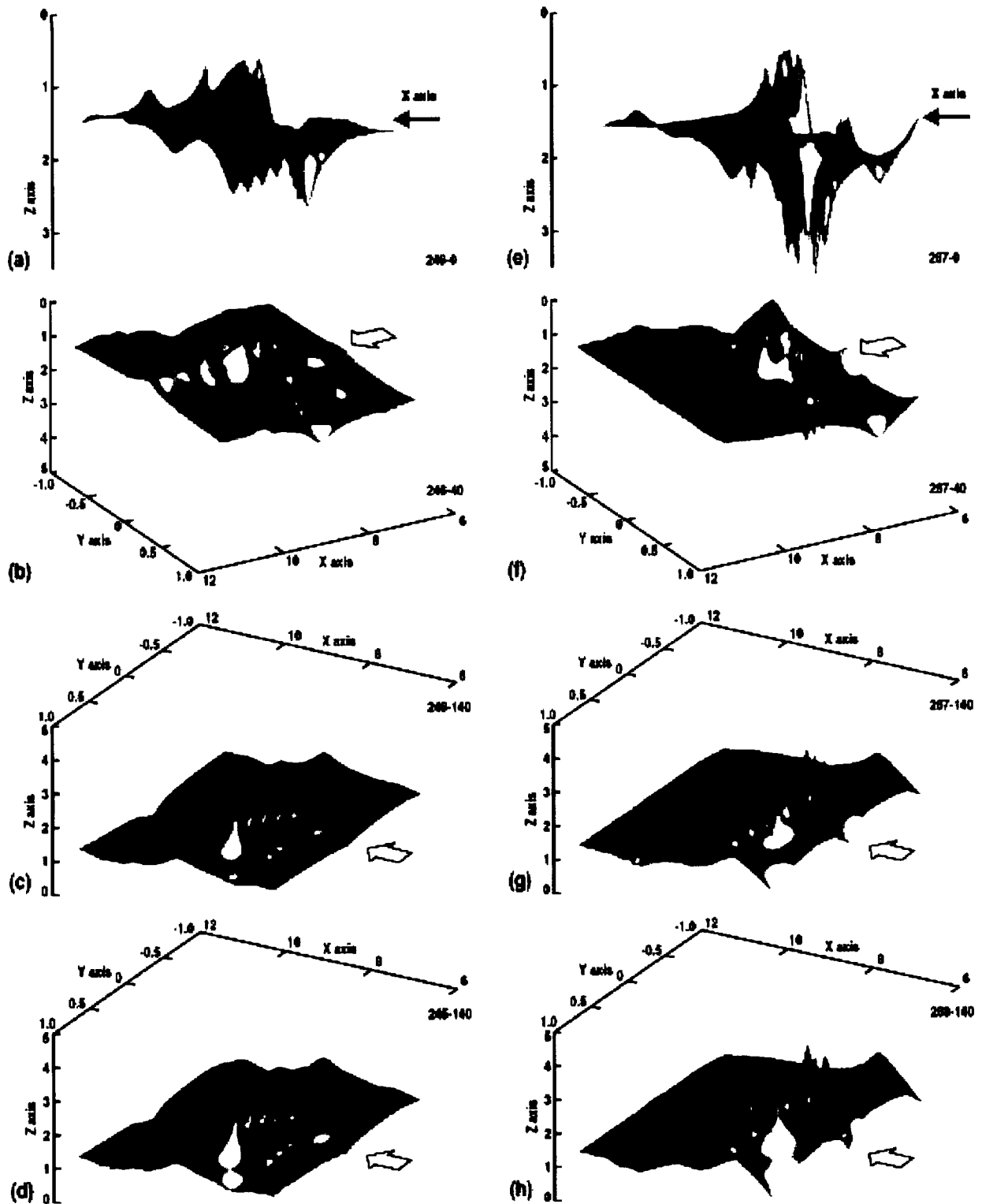


Fig. 4 - Config. 1 (0.25" hole)[RDG 267] and Config. 3 (7° half angle wedge)[RDG 246] 42.5 psia matched air injection to tunnel total pressure static pressure plots; 0°, 40°, -140° views about X axis; (a-c) Config. 3; (e-g) Config. 1; (d) Config. 3 (wedge) [RDG 245] 62.3 psia air injection; (h) Config. 1 (0.25" hole)[RDG 268] 62.5 psia air injection.

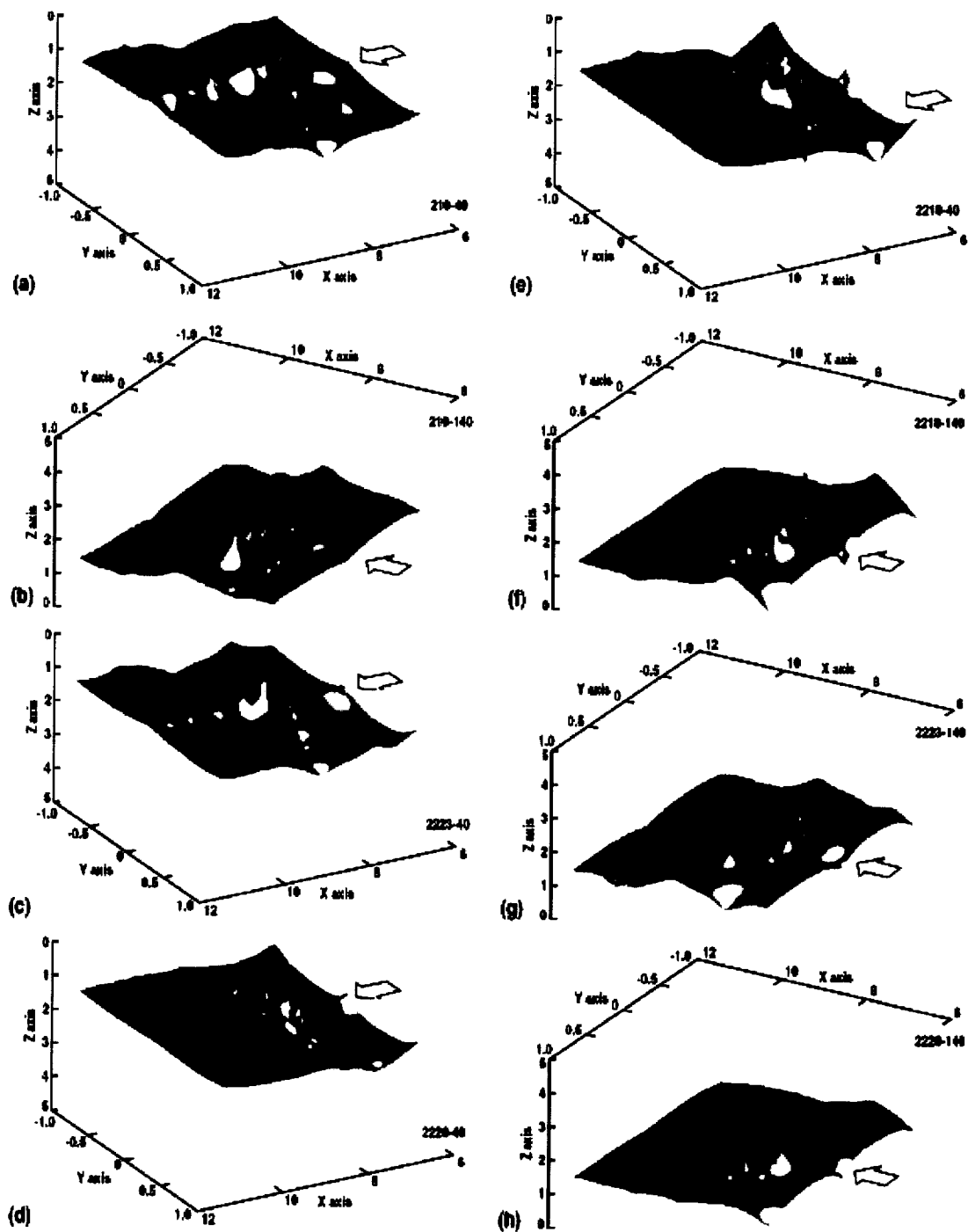


Fig. 5 -Single 42 psia helium injection comparison static pressure plots for view angles of 40° and -140° about X axis for tunnel total pressure of 42.5 psia:

Config. 3 (wedge) [RDG 210]; (a) 40°; (b) -140°;

Config. 2 (5 hole) [RDG 2223]; (c) 40°; (g) -140°;

Config. 1 (0.250" dia. hole) [RDG 2218]; (e) 40°; (f) -140°;

-Dual 56.3 psia helium injection static pressure plots; upstream Config. 1 plume onto Config. 2 plume for tunnel total pressure of 42.5 psia:

Config. 2 (5 hole) [RDG 2220]; (d) 40°; (h) -140°.

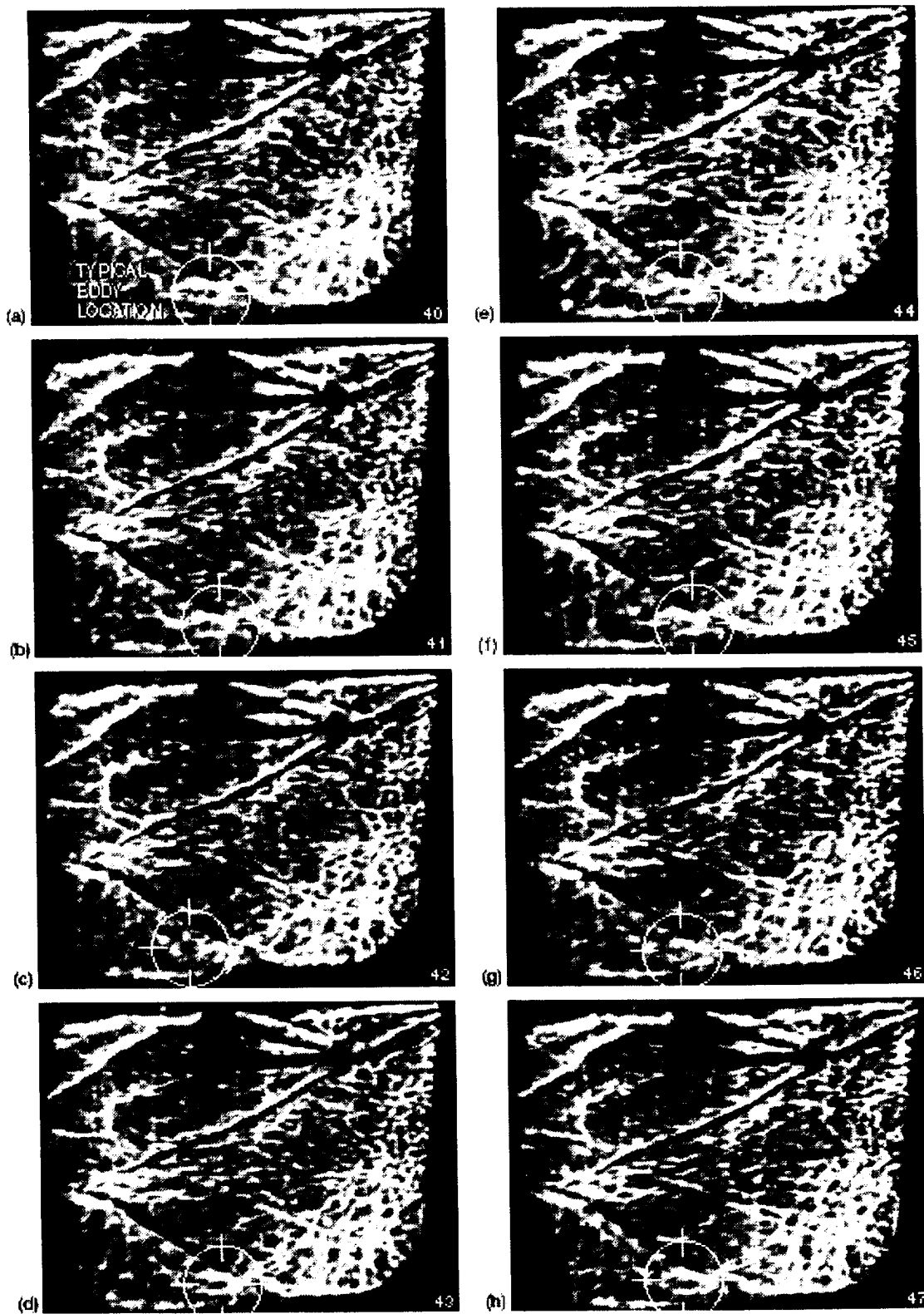


Fig. 6 - Sequential high speed video shadowgraph plume images of 22.5 psia helium injection from Config. 3 (wedge) into Mach 2.95 air flow [RDG 80]; tunnel total pressure 42.1 psia; (a) frame 40, (b) 41, (c) 42, (d) 43, (e) 44, (f) 45, (g) 46, (h) 47; typical eddy location shown by highlighted cross section in circle.

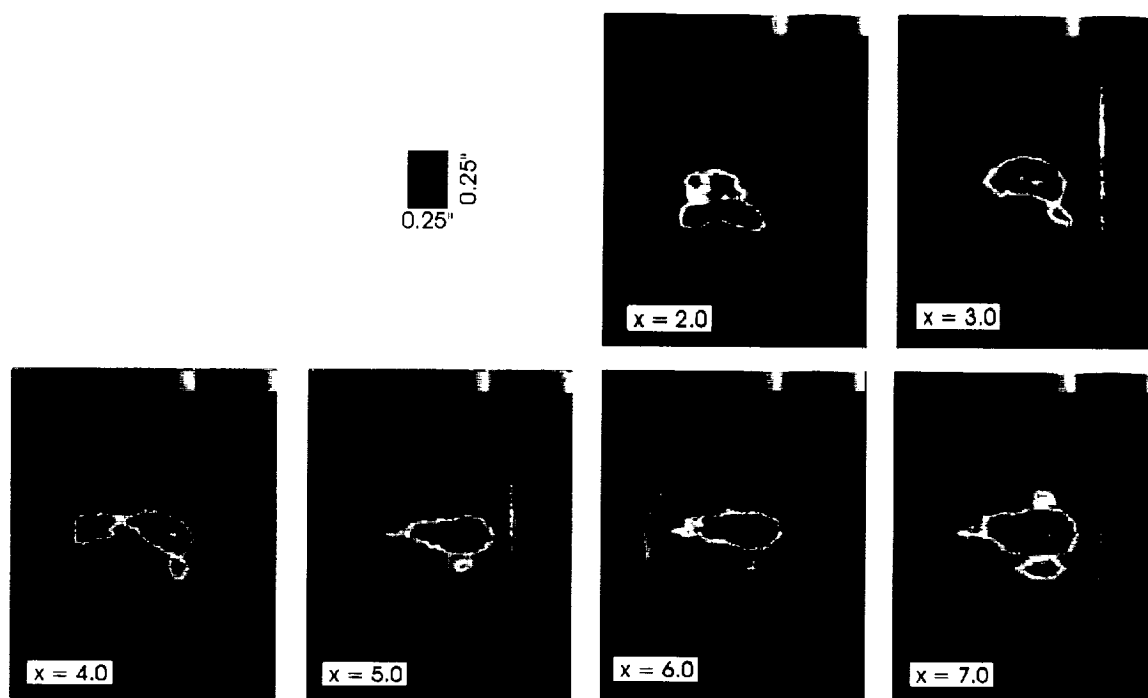


Fig. 7a - 200 (RS) image average of moist air injection from Config. 1 (0.25 inch dia. sonic nozzle) into Mach 3 crossflow; X is distance (in.) from leading edge of injector; injector and tunnel total pressure = 42.5 psia; rectangle above X = 5.0 image represents 0.25 x 0.25 inch square (shows effect of 45° viewing angle) [RDG's 262, 267, 271, 274, 277, 280]

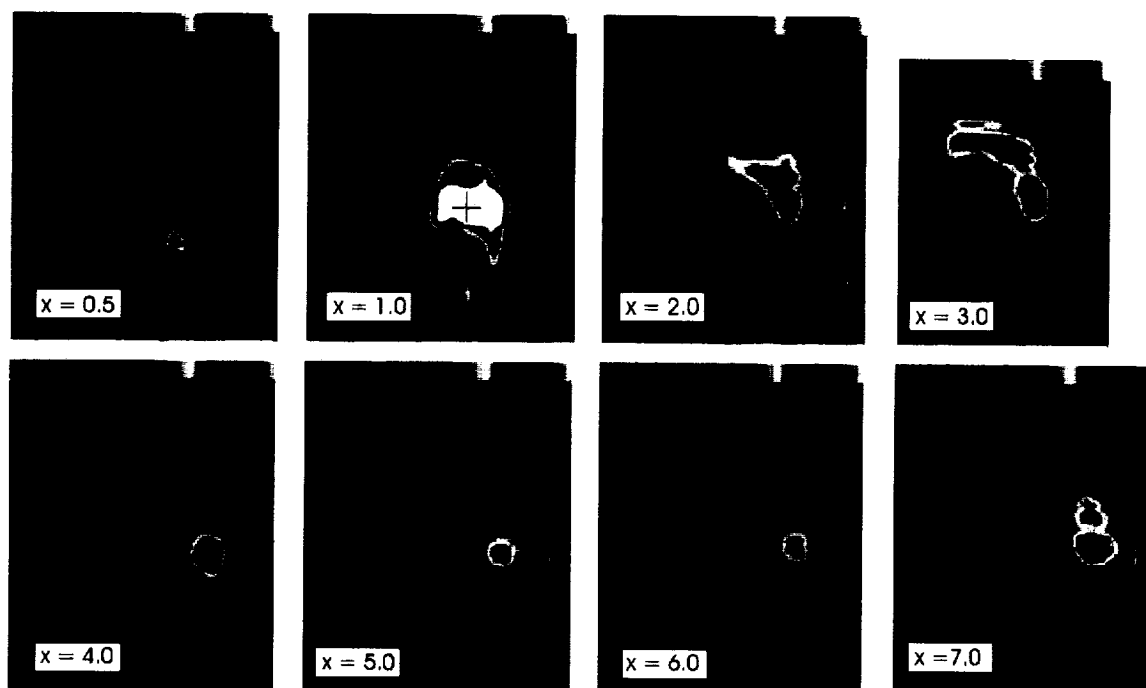


Fig. 7b - 200 (RS) image average of moist air injection from Config. 3 (wedge) into Mach 3 crossflow; X is distance (in.) from leading edge of injector; injector and tunnel total pressure = 42.5 psia [RDG 246, 239, 243, 219, 226, 230, 233, 236]

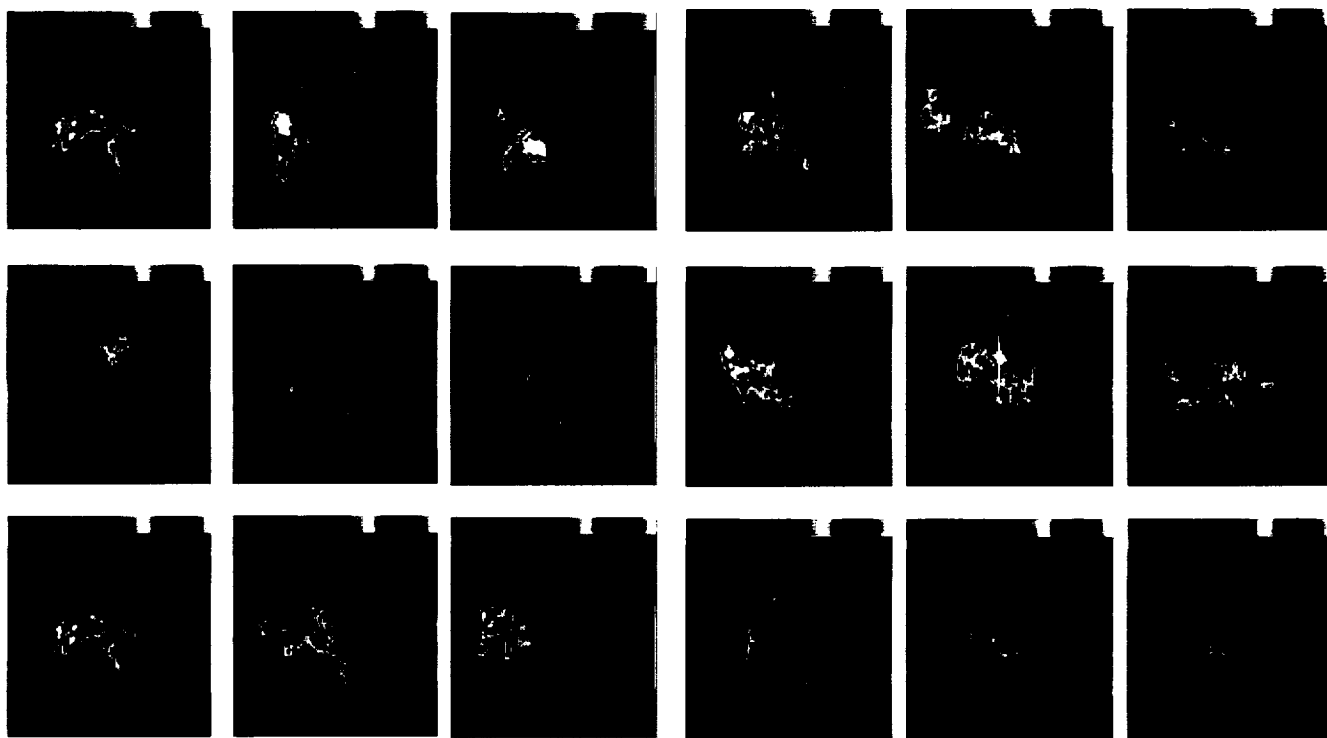


Fig.8a - Random single-shot Rayleigh scattering images of moist air injection from Config.1 (0.250 in. dia. sonic injector) [RDG 264]; injection and tunnel total pressure = 42.5 psia at $X = 2$ in. (8 diameters downstream D.P.)

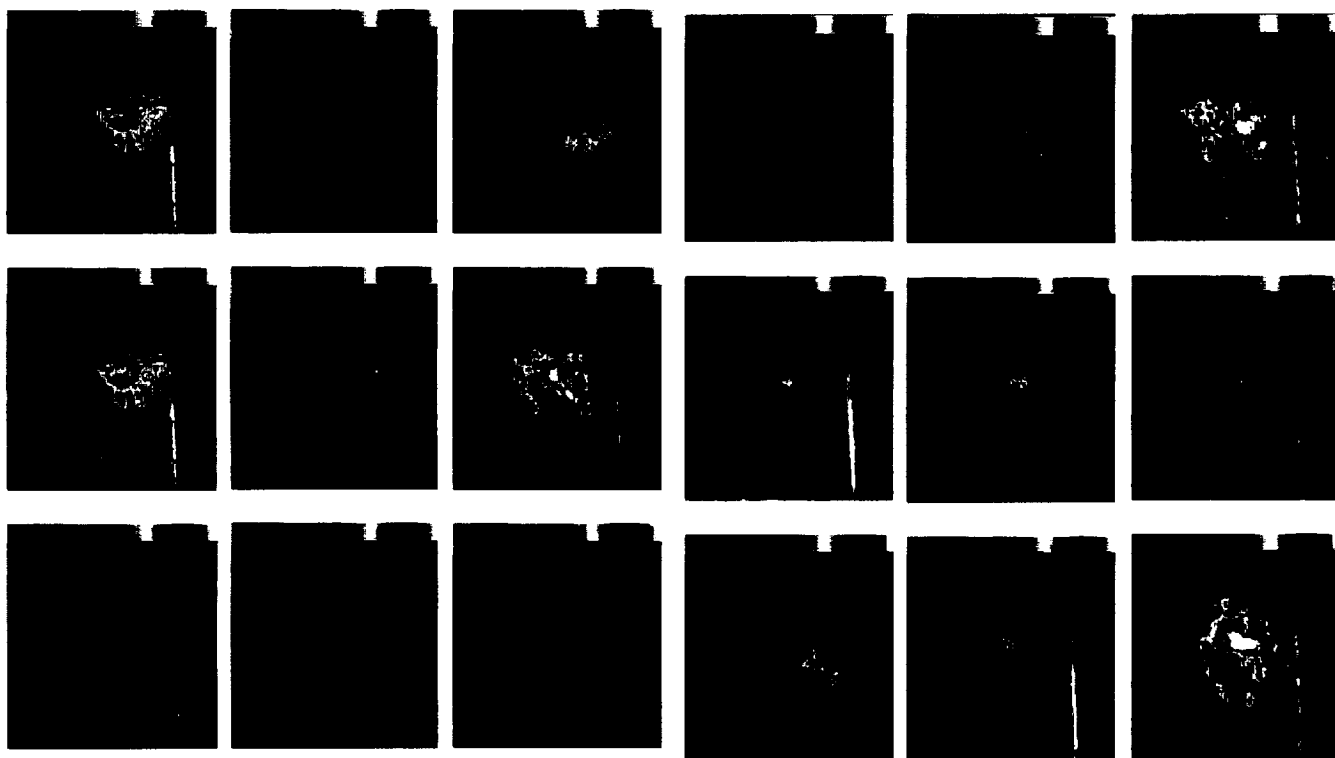


Fig.8b - Random single-shot RS images of moist air injection from Config.3 (wedge) [RDG 243]; taken at same conditions and position as figure 8a.

Videotape Supplement

The improved instrumentation/optical techniques developed to study sonic and supersonic helium or air injection/penetration into Mach 3 flow was performed in the NASA Lewis 3.81 in. by 10 in. continuous flow supersonic wind tunnel. Random single shot filtered Rayleigh scattering and high speed shadow graph video/pulse flow visualization plume images reveals several series of dynamic/unsteady flow phenomena occurring within the generated plumes. Static pressure data are shown by 3-D plots viewed rotationally about different axis for three injector designs (single 0.25 in. diameter hole, five 0.112 in. diameter holes on 0.177 in. spacing, and a 7° half angle wedge).

This 6 min video cassette supplement is a slightly lengthen version with caption titles of what was presented at the 42nd SPIE's International Symposium on Optical Science, Engineering and Instrumentation, paper 3172-52, for Optical Technology in Fluid. Thermal and Combustion Flow III at San Diego California, Convention Center, July 27–August 1, 1997.

The video supplement provides the viewer with a quick orientation of the static pressure tap distribution about each of the injector configurations. Multiple graphic interpretations of the data recorded, plus many ways to characterize the dynamic penetration of the injected gases.

The videotape supplement is available for purchase by sending the request shown below to:

NASA Center for Aerospace Information
Attn: User Services
P.O. Box 8757
Baltimore, MD 21240-0757

Date

Please send one (six minute VHS) copy of the video supplement to report
NASA TM-107533 (E-10853-V).

Name of organization

Address

City and State Zip Code

Attn.:

Title Telephone (.....)

| REPORT DOCUMENTATION PAGE | | | Form Approved OMB No. 0704-0188 | |
|---|--|--|------------------------------------|--|
| Public reporting burden for this collection of information is estimated to average 1 hour per response, including the time for reviewing instructions, searching existing data sources, gathering and maintaining the data needed, and completing and reviewing the collection of information. Send comments regarding this burden estimate or any other aspect of this collection of information, including suggestions for reducing this burden, to Washington Headquarters Services, Directorate for Information Operations and Reports, 1215 Jefferson Davis Highway, Suite 1204, Arlington, VA 22202-4302, and to the Office of Management and Budget, Paperwork Reduction Project (0704-0188), Washington, DC 20503. | | | | |
| 1. AGENCY USE ONLY (Leave blank) | 2. REPORT DATE September 1997 | 3. REPORT TYPE AND DATES COVERED Technical Memorandum | | |
| 4. TITLE AND SUBTITLE Improved Optical Techniques for Studying Sonic and Supersonic Injection Into Mach 3 Flow | | 5. FUNDING NUMBERS WU-953-74-40-00 | | |
| 6. AUTHOR(S) Alvin E. Buggele and Richard G. Seasholtz | | | | |
| 7. PERFORMING ORGANIZATION NAME(S) AND ADDRESS(ES) National Aeronautics and Space Administration Lewis Research Center Cleveland, Ohio 44135-3191 | | 8. PERFORMING ORGANIZATION REPORT NUMBER E-10853 | | |
| 9. SPONSORING/MONITORING AGENCY NAME(S) AND ADDRESS(ES) National Aeronautics and Space Administration Washington, DC 20546-0001 Marshall Space Flight Center Huntsville, Alabama 35812 | | 10. SPONSORING/MONITORING AGENCY REPORT NUMBER NASA TM-107533 | | |
| 11. SUPPLEMENTARY NOTES Prepared for the 42nd International Society for Optical Engineering Conference sponsored by the Society of Photo-Optical Instrumentation Engineers San Diego, California, July 27—August 1, 1997. To view eight segments of the supplemental video revealing dynamic/unsteady flow phenomena occurring within the generated plumes (includes random single shot filtered Rayleigh scattering (RS) plume cross section cut images, pulse and continuous light source shadowgraph, still photograph and 1000 frame per second high speed video, injector experiment, static pressure tap (RS) data gathering orientation, and several ways of displaying the 3-D pressure plots with different graphic packages). Address internet http://www.lerc.nasa.gov/WWW/AFED/research/index.html . A 12 minute video (E-10853-V) is available which provides the viewer with a quick orientation of the static pressure tap distribution about each of the injector configurations. Multiple graphic interpretations of the data recorded, plus many ways to characterize the dynamic penetration of the injected gases. Responsible person for internet representation; Mary Vickerman, organization code 1350, (216) 433-5067. Responsible person for (RS) data; Richard G. Seasholtz, organization code 5520, (216) 433-3754. Responsible person for all other data, Alvin E. Buggele, organization code 7565, (216) 433-5675/5561. | | | | |
| 12a. DISTRIBUTION/AVAILABILITY STATEMENT Unclassified - Unlimited Subject Category 35 This publication and video are available from the NASA Center for AeroSpace Information, (301) 621-0390. | | 12b. DISTRIBUTION CODE | | |
| 13. ABSTRACT (Maximum 200 words) Filtered Rayleigh Scattering and shadowgraph flow visualization were used to characterize the penetration of helium or moist air injected transversely at several pressures into a Mach 3 flow in the NASA Lewis 3.81 inch by 10 inch continuous flow supersonic wind tunnel. This work is in support of the LOX (liquid oxygen) Augmented Nuclear Thermal Rocket program. The present study used an injection-seeded, frequency doubled Nd:YAG pulsed laser to illuminate a transverse section of the injectant plume. Rayleigh scattered light was passed through an iodine absorption cell to suppress stray laser light and was imaged onto a cooled CCD camera. The scattering was based on condensation of water vapor in the injectant flow. Results are presented for various configurations of sonic and supersonic injector designs mounted primarily in the floor of the tunnel. Injectors studied include a single 0.25 inch diameter hole, five 0.112 inch diameter holes on 0.177 inch spacing, and a 7° half angle wedge. High speed shadowgraph flow visualization images were obtained with several video camera systems. Roof and floor static pressure data are presented several ways for the three configurations of injection designs with and without helium and/or air injection into Mach 3 flow. | | | | |
| 14. SUBJECT TERMS Sonic injection; Supersonic injection; Plume penetration; Mach 3 flow; Filtered Rayleigh scattering; SWT; Baseline 0.25 inch diameter sonic hose; Injector; Wedge injector and five sonic hole injector; Flow visualization; Plume geometry; Injector hot spot potential locations | | 15. NUMBER OF PAGES 20 | | |
| | | 16. PRICE CODE A03 | | |
| 17. SECURITY CLASSIFICATION OF REPORT Unclassified | 18. SECURITY CLASSIFICATION OF THIS PAGE Unclassified | 19. SECURITY CLASSIFICATION OF ABSTRACT Unclassified | 20. LIMITATION OF ABSTRACT | |